INDUCED ELECTROMAGNETIC FORCES OF LIGHTNING CURRENT CONDUCTED IN COMPOSITE LAMINATES

by

Zhi-Qiang LIU[a,b*], Sheng-Yang NIE[a], Yin WANG[a], Fu-Sheng WANG[c], and Xiu XIONG[b]

[a] Department of Engineering Mechanics, School of Civil Engineering and Architecture, Xi'an University of Technology, Xi'an, China
[b] Xi'an Airborne Electromagnetic Technology Co., Ltd., Xi'an, China
[c] Advanced Materials Testing Center, School of Mechanics, Civil Engineering and Architecture, Northwestern Polytechnical University, Xi'an, China

Original scientific paper
https://doi.org/10.2298/TSCI2502287L

The impact of electromagnetic forces induced by lightning current under lightning-induced magnetic fields when lightning strikes to composite laminates was analyzed systematically. The study especially focused on the structural responses induced by electromagnetic forces, which result from the interaction of conducting lightning currents within laminates and their self-inductance magnetic fields. It was observed that the electromagnetic forces predominantly influenced the structural responses in the vicinity of the lightning attachment region, while its influence on the responses distant from the lightning attachment region was minimal or negligible. Otherwise, the structural responses of the composite laminates remained exceedingly weak in comparison the mechanical properties of the laminates, and thus, could not cause damage to the laminates.

Key words: *electromagnetic force, lightning strike, composite laminates, coupling analysis*

Introduction

Polymer-matrix composites are extensively employed due to their exceptional specific strength and stiffness, as well as their outstanding designability, highly structured integration, *etc.* [1, 2]. However, these materials are vulnerable to lightning environment [3]. Complex structural responses can emerge in composites, including responses triggered by forces, known as electromagnetic force or Lorentz ponderomotive force [4, 5], caused by the interaction of lightning current and electromagnetic field [6].

The research referenced has explored the mechanical properties of composites under electromagnetic fields. Theoretic models were established to analyze the mechanical response of current-carrying composite plates under an electromagnetic field [4], revealing that the influence of an electromagnetic field is significant, and the deformation of the composite plate cannot be neglected. However, responses exhibited by composite laminates subjected to lightning strikes, and interaction between electromagnetic force and magnetic field of lightning, were not investigated.

* Corresponding author, e-mail: lzq537@xaut.edu.cn

A series of studies were carried out delving into the impact of electromagnetic forces on responses of composite laminates when subjected to lightning strikes. The electromagnetic field surrounding laminates during such strikes can be divided into two distinct types: field induced by lightning channel and field induced by conducting current in laminates. The response of composite laminates only considering the later was discussed in this work, and majorly investigated the impact of electromagnetic forces on the response of laminates.

Electromagnetic force in composite laminates

Figure 1 illustrates the electromagnetic field surrounding composite laminates upon lightning strikes. The I_0 is a current source in the lightning channel. The $B_{0\theta}$ is induced magnetic flux density of I_0, θ denotes the circumferential direction in the cylindrical co-ordinate system. $I_{i,z}$ is the total current of the i^{th} layer injected from the channel. The J_i is a distribution of current density in the i^{th} layer, $I_{i,z}$ is integration of J_i, over the i^{th} layer, and magnetic flux density $B_{i\theta}$ is induced by $I_{i,z}$ in the i^{th} layer. Figure 1(b) illustrates the distribution of current density within the i-th unidirectional layer [7-9]. The circular region can be considered as a minor portion relative to the entire plate surface. The current density outside away from this circular region can be referred to as the point current source.

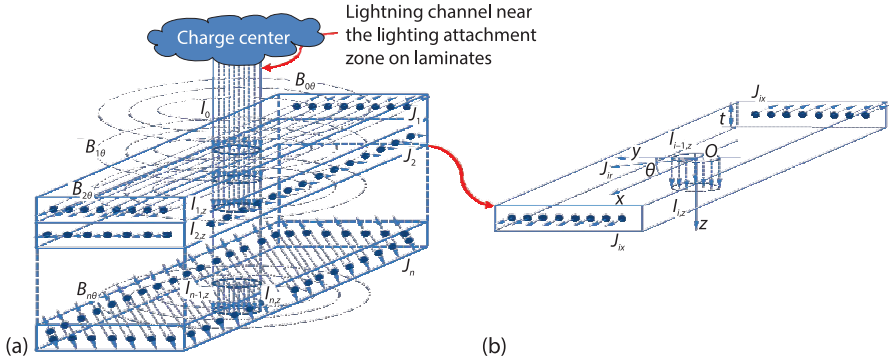

Figure 1. Electromagnetic field around composite laminates when struck by lightning

The electromagnetic force per unit mass $\boldsymbol{F}_i^L$ [7-9] generated by the lightning current J_i flowing through the fiber-reinforced unidirectional plate, which exhibits electrical anisotropy in the induced magnetic field $B_{i\theta}$, can be expressed:

$$\boldsymbol{F}_i^L = \rho_e\left(\boldsymbol{E}_e + \frac{\partial \boldsymbol{u}}{\partial t}\times \boldsymbol{B}_{i\theta}\right) + \left[\boldsymbol{\sigma}\left(\boldsymbol{E}_e + \frac{\partial \boldsymbol{u}}{\partial t}\times \boldsymbol{B}_{i\theta}\right)\right]\times \boldsymbol{B}_{i\theta} + \\ + \left\{\left[\left(\boldsymbol{\varepsilon} - \varepsilon_0 \boldsymbol{1}\right)\boldsymbol{E}_e\right]\times \boldsymbol{B}_{i\theta}\right\}_\alpha \nabla\left(\frac{\partial \boldsymbol{u}}{\partial t}\right)_\alpha + (\boldsymbol{J}_i \times \boldsymbol{B}_{i\theta}) \tag{1}$$

where $\boldsymbol{E}_e$ *is* the electric field intensity is influenced by the superposition of the discharge channel's electric field and the electric field generated by the charge on the composite plate, $\boldsymbol{\sigma}$ – the electrical conductivity tensor, ρ_e – charge density, $\boldsymbol{\varepsilon}$ – the electrical permittivity tensor, ε_0 – permittivity in the vacuum, $\boldsymbol{1}$ – the unit tensor of the second order, $\boldsymbol{u}$ – the displacement vector, and ∇ – the gradient operator, and α – the index of Einstein's summation convention.

Computational flow and material parameters

Material parameters and current values

Throughout the entire analysis process, it is crucial to take into account the relative magnetic permeability of air, the resistivity of plasma in the lightning channel, and the resistivity of composite laminates. These values are listed in tabs. 1 and 2 [10-14]. Furthermore, the mechanical properties and thermodynamic parameters of laminates are listed in tab. 3 [15]. The *RX* is longitudinal resistivity along fiber axis, *RY* is transverse resistivity perpendicular to the fiber direction within a plane, and *RZ* is through-thickness resistivity. The K_x, K_y, and K_z are thermal conductivities along the longitudinal axis, transverse axis, and through-thickness axis, respectively, C is the specific heat, and ρ – the density. The relative permeability of air is equal to 1. The elastic moduli in longitudinal, transverse, and through-thickness directions are E_x, E_y, and E_z. The μ_{xy}, μ_{yz}, and μ_{xz} denote the Poisson's ratios. The G_{xy}, G_{yz}, and G_{xz} represent the shear moduli. The *ALPX*, *ALPY*, and *ALPZ* are the thermal expansion coefficients.

Table 1. Resistivities of composite laminates [10, 11]

Temperature [°C]	27	127	227	327	427	457	527	627	727	827	3316
RX [μΩm]	62.2	59.5	56.8	54.4	52.0	51.4	49.9	48.0	46.3	44.6	134.4
RY, *RZ* [Ωm]	0.356	0.336	0.320	0.304	0.291	0.055					

Table 2. Density, specific heat, and thermal conductivities of composite laminates [12-14]

Temperature [°C]	25	330	360	500	525	815	3316
K_x [$Wm^{-1}°C^{-1}$]	11.8	6.02	5.46	2.8	2.33	1.4	1.4
K_y, K_z [$Wm^{-1}°C^{-1}$]	0.609	0.31	0.28	0.14	0.12	0.072	0.072
C [$Jkg^{-1}°C^{-1}$]	1065	2050	4250	4200	1800	1850	2300
ρ [kgm^{-3}]	1520			1170			

Table 3. Mechanical and thermal dynamic properties of composite laminates [15]

Temperature [°C]	E_x	E_y, E_z	μ_{xy}, μ_{yz}, μ_{xz}	G_{xy}, G_{xz}	G_{yz}	*ALPX*	*ALPY, ALPZ*
	[GPa]			[GPa]		[$°C^{-1}$]	
25	137	8.2	0.34	4.36	3	$1.8 \cdot 10^{-8}$	$2.16 \cdot 10^{-5}$
200	137	6.56		3.488	2.4	$5.4 \cdot 10^{-8}$	$3.78 \cdot 10^{-5}$
260	137	0.082		0.03488	0.024	$5.4 \cdot 10^{-8}$	$3.78 \cdot 10^{-5}$
600	137	0.0041		0.001744	0.0012	$5.4 \cdot 10^{-8}$	$3.78 \cdot 10^{-5}$
3316	137	0.0041		0.001744	0.0012	$5.4 \cdot 10^{-8}$	$3.78 \cdot 10^{-5}$
3317	1.37	0.00041		0.0001744	0.00012	$5.4 \cdot 10^{-8}$	$3.78 \cdot 10^{-5}$

The current values of each calculation step for lightning current waveform *A* were enumerated in tab. 4 [15].

Table 4. Parameters of lightning current waveform *A f*or every load step [15]

Load step	1	2	3	4	5	6	7	8	9	10	11	12
Time [μs]	0.489	9.78	16.3	19.6	24.5	32.6	45.7	57.1	81.5	114	179	245
Current [kA]	2.20	22.7	24.9	24.6	23.3	20.2	15.4	12.0	6.87	3.28	0.75	0.17

Computational flowchart and steps

Based on the electromagnetic field analysis of composite laminates in a lightning environment, the electromagnetic-thermal-structural coupling problem of laminates can be addressed using the decoupling method. As illustrated in fig. 2, the decoupling computational process is outlined in a flowchart, with the FE model shown in fig. 2(b).

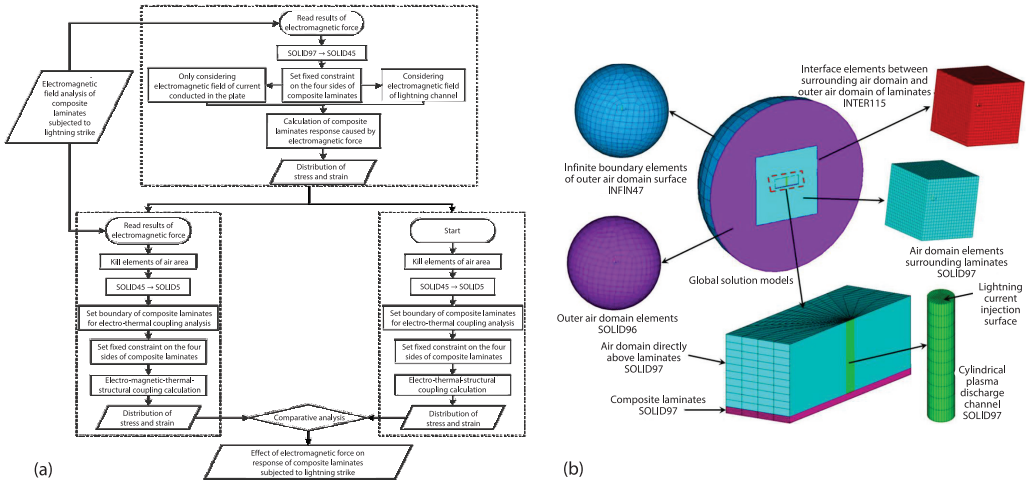

Figure 2. Electromagnetic-thermal-structural coupling analysis process of a lightning strike

Results and discussion

The influence of the self-induced electromagnetic forces on stress distribution of the plate

Figure 3(a) displays the Mises stress distribution after each load step. The Mises stress at the central node of a top surface and the maximum Mises stress on the top surface are graphically represented as lightning current varies at the end of each load step in fig. 3(b).

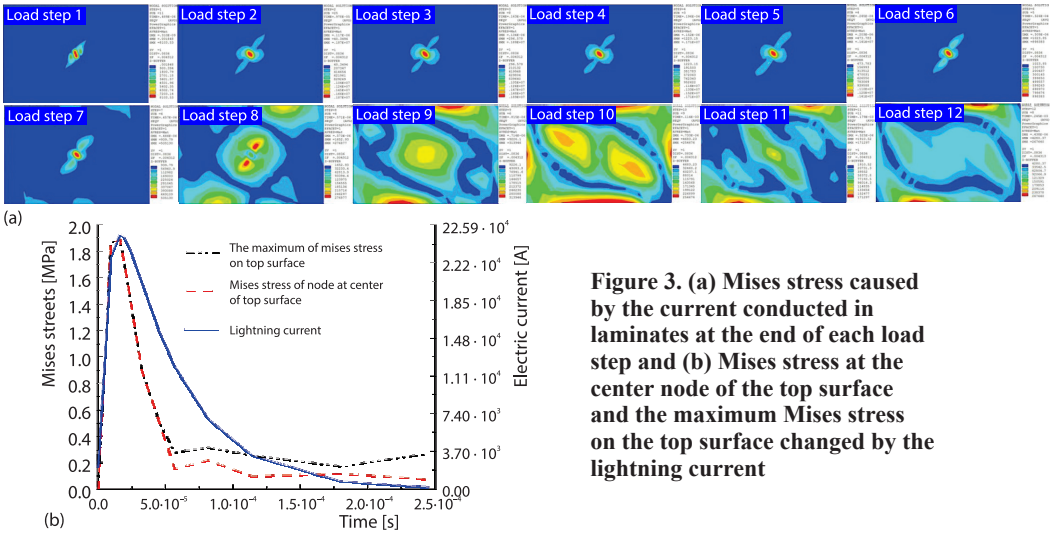

Figure 3. (a) Mises stress caused by the current conducted in laminates at the end of each load step and (b) Mises stress at the center node of the top surface and the maximum Mises stress on the top surface changed by the lightning current

As observed in fig. 3(a), although the value of the Mises stress for the initial seven load steps exhibits significant variation, the distribution form remains relatively unchanged. A significant transformation in Mises stress distribution becomes apparent starting from the 8th load step, with the maximum value no longer being centered. As illustrated in fig. 3(b), the Mises stress on the top surface at each load step does not exceed 2 MPa, indicating that they would not lead to damage in composite laminates.

The influence of the self-induced electromagnetic forces on the displacement of the plate

The distribution of displacements u_z at the end of each load step, parallel to the initial top surface's normal direction, was presented in fig. 4(a). In fig. 4(b), the displacements u_z of six pre-defined paths are depicted against the variation of lightning current. The pre-defined paths were delineated in fig. 4(c), with red arrows indicating their respective directions. The PATH-5 is situated at the core of the middle section of the laminates, while PATH-6 is situated at the periphery of the circular area on the top surface of the laminates.

Figure 4(a) demonstrates that displacements in z-direction assume both positive and negative values during the initial nine load steps, suggesting a slight buckling of the top layer. The dominant direction of buckling deformations is along the −45° axis, as inferred from the

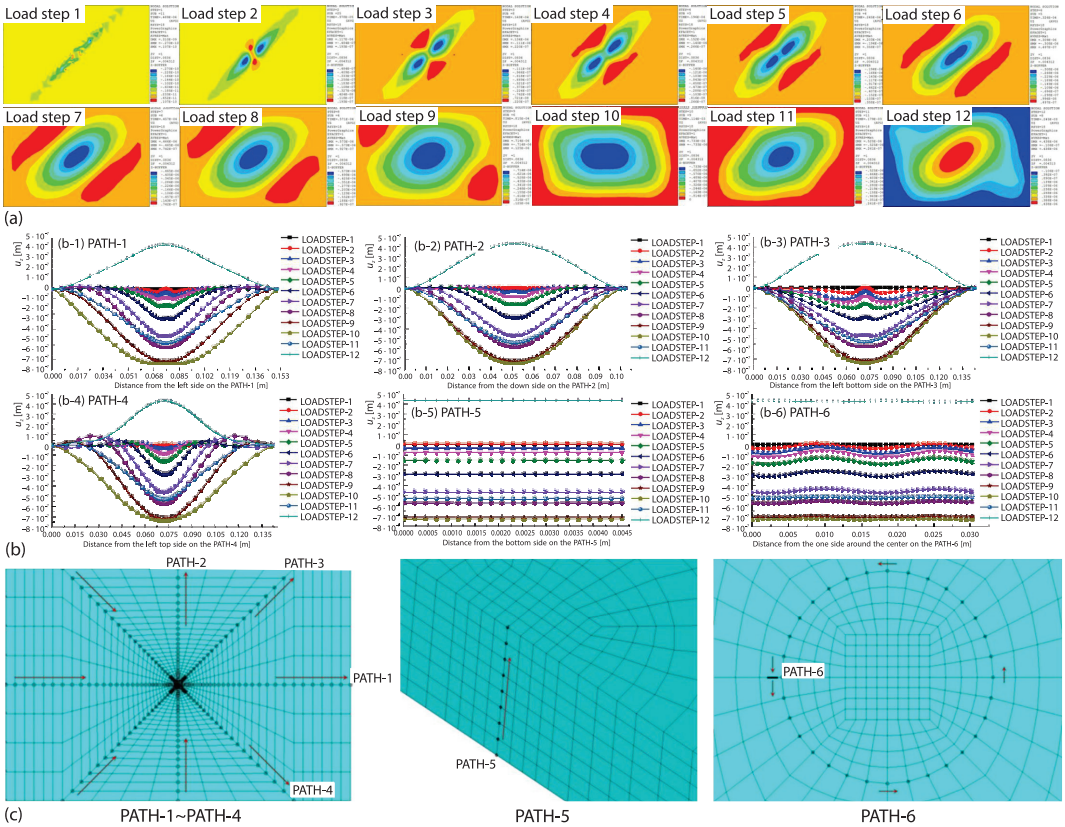

Figure 4. (a) Distribution of u_z caused by current conducted in laminates at end of each load step, (b) displacement u_z of each path caused by current conducted in laminates at end of each load step, and (c) predefined paths

fourth graph in fig. 4(b). The prominent deflections are primarily observed within the central region of composite laminates, as illustrated in fig. 4(a) and PATH-1 to PATH-4 in fig. 4(b). The laminates exhibit negative *z*-directional deflections prior to completion of the 10th load step, with deflections incrementally escalating over time. Following the 11th load step, there was a gradual reduction in deflections along the negative *z*-direction. Subsequently, these deflections reversed, leading to deflections in positive *z*-direction for laminates. By the end of the lightning current load, the laminates exhibit their maximum deflection in the positive *z*-direction. The consistent displacement of every point in the thickness direction at the center of the laminates, as observed from the fifth graph in fig. 4(b), suggests the absence of discontinuous deformation at the position of laminates. The *z*-direction displacements of the top layer of laminates at any given moment are less than 0.8 μm, exceedingly minimal.

Conclusion

The influence of electromagnetic forces on the response of composite laminates in a lightning environment was analyzed based on electromagnetic field analysis. Responses of laminates caused by electromagnetic forces generated solely by the electromagnetic fields induced by the lightning current within the composite laminates were discussed in this work. The process of electromagnetic field analysis of composite laminates can carry out the whole process of lightning strikes to laminates. Results suggest that when considering the electromagnetic field induced only by lightning current conducted in composite laminates, the electromagnetic forces impact the laminates' response feebly. This impact can be negligible compared to the mechanical properties of the laminates and cannot cause damage. The rest of the results acquired in this analysis process will be shown and discussed in subsequent articles.

Acknowledgment

This work was supported by the National Natural Science Foundation of China (52175147) and the Aviation Science Foundation of China (20200044053002).

Nomenclature

ALP – thermal expansion coefficient, [1/°C]
$\boldsymbol{B}$ – magnetic flux density vector, [T]
C – specific heat, [Jkg^{-1}°C^{-1}]
E – elastic moduli, [GPa]
$\boldsymbol{E}_e$ – electric field intensity vector, [Vm^{-1}]
$\boldsymbol{F}^L$ – electromagnetic force, [Nkg^{-1}]
G – shear moduli, [GPa]
I – electric current, [A]
J – electric current density, [Am^{-2}]
K – thermal conductivity, [Wm^{-1}°C^{-1}]
R – electrical resistivity, [Ωm]
$\boldsymbol{u}$ – displacement vector, [m]
X, x – fiber direction, [–]
Y, y – transverse direction perpendicular to fiber direction within a plane, [–]
Z, z – through-thickness direction, [–]

Greek symbols

α – index of Einstein's summation convention
$\boldsymbol{\varepsilon}$ – electrical permittivity tensor, [Fm^{-1}]
θ – circumferential angle, [rad]
μ – Poisson's ratios, [–]
ρ – density, [kgm^{-3}]
ρ_e – charge density, [Cm^{-3}]
$\boldsymbol{\sigma}$ – electrical conductivity tensor, [Sm^{-1}]

References

[1] Li, Y., *et al*., Impact Damage Reduction of Woven Composites Subject to Pulse Current, *Nature Communications*, *14* (2023), ID5046
[2] Guo, Y. L., *et al*., Eliminating Lightning Strike Damage to Carbon Fiber Composite Structures in Zone 2 of Aircraft by Ni-Coated Carbon Fiber Non-woven Veils, *Composites Science and Technology*, *169* (2019), Jan., pp. 95-102
[3] Millen, S. L. J., *et al.*, Modelling and Analysis of Simulated Lightning Strike Tests: A Review, *Composite Structures*, *274* (2021), ID114347

[4] Barakati, A., *et al*., Influence of the Electric Current Waveform on the Dynamic Response of the Electrified Composites, *International Journal of Mechanics and Materials in Design*, *9* (2013), 1, pp. 11-20
[5] Kumar, V., *et al.*, Factors Affecting Direct Lightning Strike Damage to Fiber Reinforced Composites: A Review, Composites Part B, *Engineering*, *183* (2020), ID107688
[6] Chernikov, D., *et al*., Optimization of Dynamic Mechanical Response of a Composite Plate Using Multi-field Coupling with Thermal Constraints, *Applied Mathematical Modelling*, *58* (2018), June, pp. 19-32
[7] Todoroki, A., *et al*., Effect of Dents in Laminated Carbon Composite Beams on Modified Anisotropic Electric Potential Analysis, *Composite Structures*, *200* (2018), Sept., pp. 340-345
[8] Barakati, A., *et al*., Mechanical Response of Electrically Conductive Laminated Composite Plates in the Presence of an Electromagnetic Feld, *Composite Structures*, *113* (2014), July, pp. 298-307
[9] Zhupanska, O. I., *et al.*, Electro-Thermo-Mechanical Coupling in Carbon Fiber Polymer Matrix Composites, *Acta Mechanica*, *218* (2011), Dec., pp. 319-332
[10] Liu, Y. K., *et al*., Modelling the Lightning Continuing Current Electric Arc Discharge and Material Thermal Damage: Effects of Combinations of Amplitude and Duration, *International Journal of Thermal Sciences*, *162* (2021), 106786
[11] Lago, F., *et al*., A Numerical Modelling of an Electric Arc and Its Interaction with the Anode: Part III, Application the Interaction of a Lightning Strike and an Aircraft in Flight, *Journal of Physics D: Applied Physics*, *39* (2006), 10, pp. 2294-2310
[12] Dong, Q., *et al*., Damage Analysis of Carbon Fiber Composites Exposed to Combined Lightning Current Components D and C, *Composites Science and Technology*, *179* (2019), July, pp. 1-9
[13] Abdelal, G., *et al.*, Non-Linear Numerical Modelling of Lightning Strike Effect on Composite Panels with Temperature Dependent Material Properties, *Composite Structures*, *109* (2014), Mar., pp. 268-278
[14] Wang, Z. H., *et al*., Development of Laser Processing Carbon-Fiber-Reinforced Plastic, *Sensors*, *23* (2023), 7, 3659
[15] Liu, Z. Q., *et al*., Combining Analysis of Coupled Electrical-Thermal and BLOW-OFF Impulse Effects on Composite Laminate Induced by Lightning Strike, *Applied Composite Materials*, *22* (2014), June, pp. 189-207

Paper submitted: October 12, 2024
Paper revised: November 25, 2024
Paper accepted: Decenber 3, 2024